Advanced Fiber Materials (2023) 5:1076–1087
https://doi.org/10.1007/s42765-023-00269-5

RESEARCH ARTICLE

Water Responsive Fabrics with Artificial Leaf Stomata

Lihong Lao[1,2] · **Hedan Bai**[3,4] · **Jintu Fan**[1,5]

Received: 15 October 2022 / Accepted: 31 January 2023 / Published online: 8 March 2023

Abstract
Due to fiber swelling, textile fabrics containing hygroscopic fibers tend to decrease pore size under wet or increasing humidity and moisture conditions, the reverse being true. Nevertheless, for personal thermal regulation and comfort, the opposite is desirable, namely, increasing the fabric pore size under increasing humid and sweating conditions for enhanced ventilation and cooling, and a decreased pore size under cold and dry conditions for heat retention. This paper describes a novel approach to create such an unconventional fabric by emulating the structure of the plant leaf stomata by designing a water responsive polymer system in which the fabric pores increase in size when wet and decrease in size when dry. The new fabric increases its moisture permeability over 50% under wet conditions. Such a water responsive fabric can find various applications including smart functional clothing and sportswear.

Keywords Breathable fabric · Fabric pores · Hydrogel · Leaf stomata · Water responsive

Introduction

Smart responsive textiles that regulate their structure and properties according to external stimuli such as moisture and temperatures are attracting increasing attention for various applications [1–4]. In such textiles, it is highly desirable, for example, to increase the opening of fabric pores under humid and sweating conditions so as to maximize ventilation and cooling, while closing the pores under cold and dry conditions for increased heat retention and barrier protection. Such a behavior is, however, contrary to that of the conventional fabric which generally have reduced pore size under wet conditions due to fiber swelling and increased pore size under dry conditions.

There have been many attempts to create such an unconventional fabric behavior. For example, Zhong et al. [5] and Mu et al. [6] created pre-cut flaps in patterned Nafion™, a perfluorosulfonic acid ionomer (PFSA)-based films, which opened in high humidity. More recently, other materials have been used to construct moisture sensitive flaps for modulating ventilation in clothing. For example, Wang et al. [7] constructed a heterogeneous biohybrid film, comprising a humidity-sensitive layer of special living cells and a humidity-insensitive layer; Kim et al. [8] developed a bilayer moisture-responsive actuator comprising a hydrophobic polyethylene terephthalate (PET) layer and hygroscopic cellulose acetate (CA)/polyethylene glycol (PEG) layer; Li et al. [9] developed a three-layer moisture-responsive film comprising nylon, silver (Ag) and polystyrene-poly(ethylene-ran-butylene)-polystyrene (SEBS) nanocomposite layers. Nevertheless, in all these attempts, all the flapping actions occurred out of the fabric planes, which adversely affected the tactile comfort and/or appearance of the clothing. Hence, Jia, Hu, Khan and Liu et al. [10–12] adopted a different approach, in which the fabric or textile changed its shape and openings with the increase of humidity via twisted and coiled artificial muscles (e.g., silk fiber and bamboo fiber) so as to enlarge the unclothed body area for cooling. Although this approach involved only the in-plane deformation, it

✉ Jintu Fan
jin-tu.fan@polyu.edu.hk

1 Department of Fiber Science & Apparel Design, Cornell University, Ithaca, NY 14853, USA

2 Present Address: Department of Materials Science and Engineering, University of Illinois Urbana-Champaign, Urbana, IL 61801, USA

3 Sibley School of Mechanical and Aerospace Engineering, Cornell University, Ithaca, NY 14853, USA

4 Present Address: Querrey Simpson Institute for Bioelectronics, Northwestern University, Evanston, IL 60208, USA

5 School of Fashion and Textiles, Hong Kong Polytechnic University, Hung Hom, Kowloon, Hong Kong, China

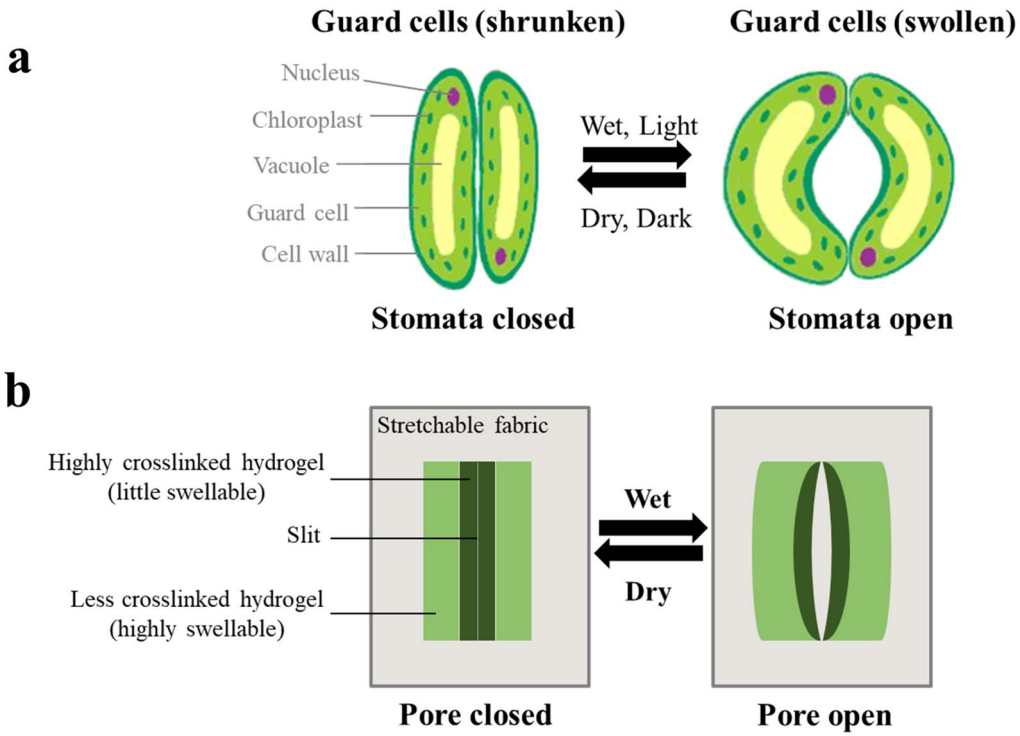

Fig. 1 Schematic illustration of the design of a stretchable fabric simulating the plant leaf stomata. **a** The opening and closing behavior of guard cells (pores) in leaf stomata. **b** The design of a stretchable fabric simulating the plant leaf stomata where the slit areas have been coated with three hydrogel layers, the inner layer and the two outer layers being composed of highly cross-linked (HC) little swellable hydrogel and less cross-linked (LC) highly swellable hydrogel, respectively. These simulated leaf stomata were assumed to open the pores/slits under wet conditions, and close the pores/slits under dry conditions

could only be used in certain garment parts, e.g., sleeves and pants.

Our present approach is different in that it involves pores (or cut slits) within the fabric enlarging or shrinking in a similar way to that which occurred in the leaf stomata of a plant (Fig. 1a). A stoma is a portal in a plant leaf which controls carbon dioxide (CO_2) exchange and water transpiration for photosynthesis and other metabolic processes [13]. It has two guard cells, with relatively inextensible thick inner walls and relatively extensible thin outer walls [14]. The stomata open and close in response to changes in the environments, such as humidity, light and CO_2 levels [15, 16]. Under high humidity (wet) or light intensities, the two guard cells swell and bend apart, creating an open pore to draw the water in; whereas the reverse is true under low levels of humidity and light, the two cells shorten, leading to closing of the pores so as to prevent a loss of water (Fig. 1a).

In the present approach, the actuation of the leaf stomata is emulated in a stretchable knitted nylon fabric by creating artificial guard cells at the edges of the cut slits using the water responsive polyacrylamide (PAAm) hydrogel at two different levels of cross-linking (Fig. 1b). Because the less cross-linked (LC) PAAm hydrogel at the outer layer of the slit swells 100 times more than that of its highly cross-linked (HC) counterpart at the inner layer when wet, the hydrogel layers (acting as artificial guard cells) bend outwards to open the slits (pores) in the fabric as the surrounding wetness increases. Unlike the "flap approach" in most previous studies [5–9], the fabric deforms within its own plane, thereby not affecting the overall appearance or the tactile comfort.

Experiments

Preparation of Polyacrylamide Hydrogel

The polyacrylamide (PAAm) hydrogels were synthesized as follows [17]. 12 wt % acrylamide (AAm; Sigma-Aldrich, A8887) aqueous monomer solution was prepared, to which a photoinitiator, Darocur® 1173 (BASF) and a cross-linker, N,N′-methylene bisacrylamide (MBA; Sigma, M7279) were subsequently added. The photoinitiator was 0.2 wt% of the solution and the cross-linker was 0.12 wt% for the less cross-linked (LC) hydrogel and 1.2 wt% for the

highly cross-linked (HC) hydrogel. To certain solutions, 1.2 wt% of PAAm polymer ($M_w \sim 5 \times 10^6$, Sigma-Aldrich, 92560) was added for a comparison [18]. After stirring the solutions at room temperature overnight, each homogeneous solution was poured into a microtome embedding mold (15 mm wide, 7 m high and 4 mm deep, Electron Microscopy Sciences) and photo-polymerized under ultraviolet (UV) light at 365 nm (UVP Blak-Ray™ B-100AP High-Intensity UV Inspection Lamps, Fisher Scientific) for 10 min.

Preparation of Three-Layer Sandwiched Hydrogel Composite

A three-layer sandwiched hydrogel composite was synthesized by curing the two hydrogel solutions in the microtome mold step-by-step, the two outer layers being composed of the less cross-linked (LC) hydrogel and the inner layer of the highly cross-linked (HC) hydrogel. For each layer, 400 µL of the solutions was used and photo-polymerized under UV light (365 nm) for 10 min. The stacking and polymerization sequence was as follows: the LC solution for the first layer, the HC solution for the second layer and another LC solution for the third (viz. final) layer.

Coating of three-layer hydrogel on slit areas of the fabrics

Knitted nylon fabrics (100% Nylon, NNP 32,003) provided by Nanjing Yuyuan Textile Co., Ltd, were first washed, and then pre-activated in a 5 wt% benzophenone (BP, Alfa Aesar, A10739)/ethanol solution [19]. To prepare the hydrogel coating, the BP pre-treated fabric was covered with a tape mask which had a patterned pore/slit groove structure. The slit area was composed of three windows, with widths of 2 mm and 2.5 mm for the inner and two outer windows, respectively, and a same height of 9 mm. Each slit area was spaced by 6 mm and 4 mm in horizontal and vertical directions, respectively. A water-based glue (Elmer's School Glue) was then pasted into the grooves of the tape mask. After the glue had solidified, the mask was peeled off to form a stoma template with three windows on the fabric. After that, 10 µL of each hydrogel solution was poured into the windows and cured in a sequence, i.e., first the HC hydrogel solution in the inner window, and then the LC hydrogel solution in the two outer windows. Afterwards, a 9-mm slit was cut with a blade in the central position of the inner HC hydrogel layer and completely through the fabric. Afterwards, the fabric was immersed in a water bath to wash out the glue, and finally dried at room temperature.

Characterizations

Morphology A scanning electron microscopy (SEM; Tescan Mira3 FESEM) was used to observe the morphology of the PAAm hydrogels having the different cross-linker loadings as well as the fabrics with and without the hydrogel coatings in the slit. The different samples were freeze-dried and coated with gold palladium before the observation.

Water uptake (swelling) and volume change of individual hydrogels Various PAAm hydrogel samples (4 mm wide, 7 mm high, and 1 mm thick) were immersed into the water for the swelling test. The samples were taken out at different times, surfaces wiped with Kimwipes™ Delicate Task Wipers and then weighed (W_t, g). The water uptake (swelling) ratio was defined as follows:

$$\frac{(W_t - W_0)}{W_0} \times 100\%, \tag{1}$$

where W_0 was the original weight (g) before the water immersion[20, 21]. The volume change was also determined by measuring the dimensions of each hydrogel sample at different times during the swelling (V_t, mm^3) with the volume expansion ratio being defined as follows:

$$\frac{(V_t - V_0)}{V_0} \times 100\%, \tag{2}$$

where V_0 was the original volume (mm^3) before immersion in the water [22].Three specimens were tested to obtain the average value.

Mechanical tests of hydrogels The mechanical properties of the two differently cross-linked PAAm hydrogels before (as-prepared) and after water swelling (for 24 h) were tested at 0.1 N/min to a maximum force of 18.0 N on a dynamic mechanical analysis (DMA) tensile tester (Q800, TA Instruments), the hydrogel samples being cut into a rectangle shape (~ 4 mm wide, 8 mm high, and 0.2 mm thick). From the obtained stress–strain curves, the Young's modulus (E, at 2.5% strain), fracture stress (σ_f) and fracture strain (ε_f) were derived by means of Universal Analysis 2000 software (TA instruments). At least three specimens were tested and their values were averaged.

Water response of hydrogels with cut slits Samples (4 mm wide, 7 mm high, and 1 mm thick) of the LC hydrogel, HC hydrogel and three-layer sandwiched hydrogel composite were cut from the cross-sections of the molded samples, and a 6-mm slit was then cut in the central position of each sample. The samples were immersed into water for 10 min at room temperature and tested their water response.

Water response of fabrics with hydrogel coated slits The fabrics with the slit areas coated with different hydrogel combinations were tested for the water response by

immersing them for 10 min in water at room temperature, the control fabric with slits only (viz. no coating) also being tested. Optical microscopy (BX51, Olympus Corporation) was used to assess the slit behavior and the slit dimensions.

Artificial sweat response of fabrics with hydrogel coated slits The slit response to artificial sweat was assessed by immersing the fabric with the optimal hydrogel coating in the slit areas into contact with the artificial sweat for 10 min at room temperature. During the first 5 min, the fabric was floated on the liquid, after which it was immersed completely in the liquid for the remaining 5 min. The fabric with slits only (viz. no coating) was also tested as a control. In both cases, videos were used to record the slit response. The artificial sweat was prepared according to the ISO 3160-2 standard, which contains 20 g/L NaCl, 17.5 g/L NH_4Cl, 5 g/L acetic acid and 15 g/L D, L-lactic acid with pH of 4.7 adjusted by NaOH [23].

Water vapor transmission rate (WVTR) The WVTR of various fabrics was measured by means of a cup method (BS 7209 standard) [24, 25], with the temperature raised to 35 °C. Various circular samples with a diameter of ~ 90 mm were cut, and then attached to the edge of standard aluminum cups via an adhesive plus a tape. Each cup was pre-filled with ~ 60 g water, with a triangular aluminum support being used to prevent the testing sample from sagging into the water. The cups were placed on a heater with a temperature of 35 °C, and mass of the water lost/evaporated through the fabric was measured after 1 h. The *WVTR* (g/m^2/h) was calculated as follows:

$$\mathrm{WVTR} = \frac{M}{At}, \tag{3}$$

where M is the water mass loss (g), A is the area of the fabric exposed to the water in the cup and is the same as the internal area of the cup (m^2), and t is the test period (h). Prior to testing, all the samples were placed in a standard atmosphere (20 ± 2 °C temperature, 65 ± 2% relative humidity) for 24 h. The results were obtained by averaging the values of three specimens.

Air permeability The air permeability of the fabrics were tested on a gas permeability module on a Capillary Flow Porometer 7.0 (CFP-1100-AEHXL, Porous Materials Inc.) [26]. Various circular samples with a diameter of ~ 25 mm were cut, and then gently placed in the chamber, and fixed by means of an O-ring (18.3 mm and 25 mm inner and outer diameters, respectively). As the fabrics were being tested, air pressure increased, and air flow and pressure drop across the samples were measured. The results of Darcy's Permeability Constant (C) was obtained by means of the associated software, calculated as follows:

$$C = \frac{8FTV}{\pi D^2\left(P^2 - 1\right)}, \tag{4}$$

where C is the Darcy's Permeability Constant (Darcy or cm^2, 1 Darcy equal to 9.87×10^{-9} cm^2), F *is* the air flow (cm^3/s), T *is* the sample thickness (mm, ~ 0.39 mm for the knitted nylon fabric), V is the air viscosity (0.0185 CP), D is the sample diameter (mm), and P is the pressure (atmospheres, psi). Prior to testing, all the samples were conditioned in a standard atmosphere (20 ± 2 °C temperature, 65 ± 2% relative humidity) for 24 h. The results were obtained by averaging the values of three specimens .

Data analysis The ANOVA was used to analyze the data with the significance level set at $p < 0.05$, and the results being given as mean ± standard deviation.

Results

Three-Layer Sandwiched Hydrogel

The polyacrylamide (PAAm) hydrogels were synthesized by means of UV photo-polymerization, with N, N'-methylene bisacrylamide (MBA) as the cross-linker [17], two hydrogels with different cross-linker loadings being prepared. The less cross-linked (LC) hydrogel, with a cross-linker loading of 0.12 wt%, appeared transparent, whereas the highly cross-linked (HC) hydrogel, with a cross-linker of 1.2 wt% appeared white (Fig. 2a), possibly as a result of the non-homogeneous gelation with relatively large amount of the cross-linker [27]. The microstructure of both hydrogels displayed an open porous morphology after freeze-drying with the HC hydrogel network being less porous than that of the LC hydrogel due to the increased cross-linker concentration (Fig. 2b) [28].

The water uptake (swelling ratio) (solid lines in Fig. 2c) and volume expansion (dashed lines in Fig. 2c) were found to be different for the two hydrogels (significance level $p < 0.05$). The LC hydrogel rapidly absorbed water and became swollen with a high deformation speed, reaching almost 130% of the original weight and 115% the original volume after 300 min, after which little further water absorption or swelling occurred; In contrast to this, the HC hydrogel showed little swelling (the images can be found in Fig. S1) and even experienced a slight decrease in weight and volume, possibly due to the water loading in the gel already being higher than that the highly cross-linked network could accommodate, leading to a rejection of the excessive water when the hydrogel reaches its equilibrium. Xu et al. [29] previously reported a similar decrease in the volume and weight of nanocomposite hydrogels when immersed in water, also attributing it to the increased cross-linking density of the hydrogels. The volume change showed a similar trend as

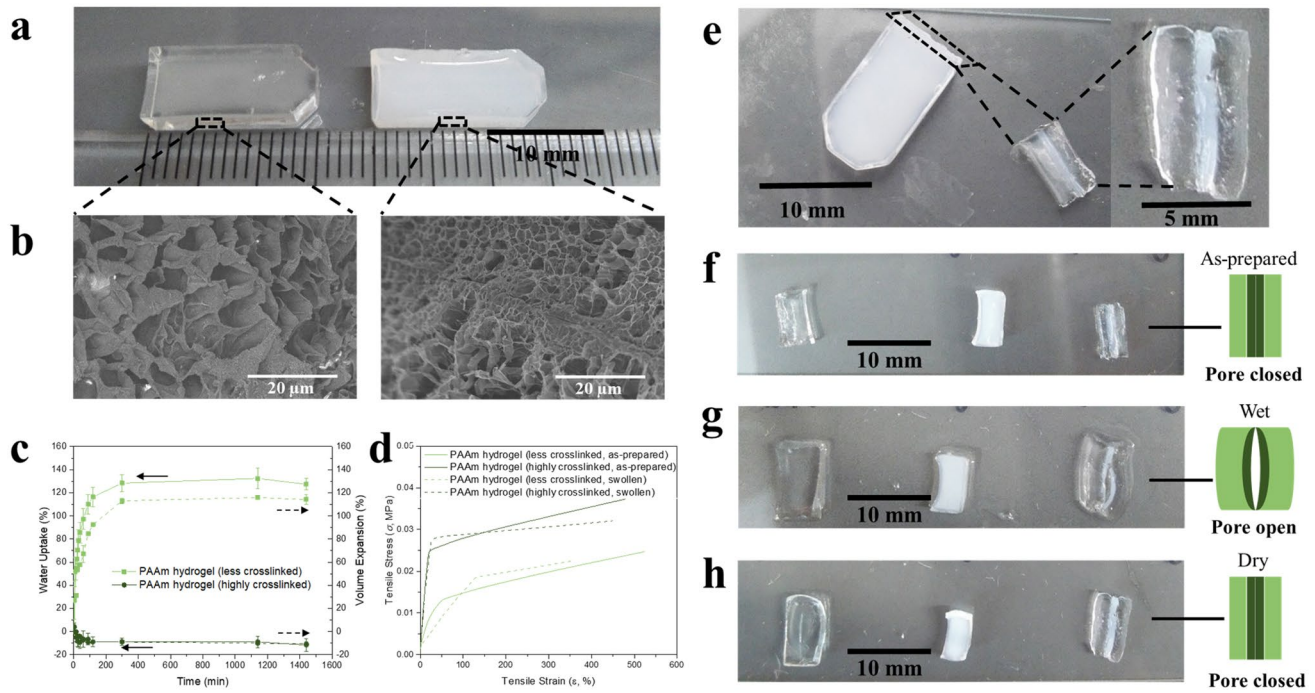

Fig. 2 Morphologies, mechanical properties and water behaviors of differently cross-linked polyacrylamide (PAAm) hydrogels and three-layer sandwiched hydrogel composite. **a** Photo and **b** SEM images of the less cross-linked (LC) (left) and highly cross-linked (HC) (right) PAAm hydrogels, respectively. **c** Water uptake (swelling ratio) and volume expansion of the two hydrogels. **d** Representative stress–strain curves of the two hydrogels before and after swelling. **e** Top and cross-sectional views of the three-layer sandwiched hydrogel composite. **f–h** Water response of the cut slits in the central position of the LC (left), HC (middle) and three-layer (right) hydrogel samples, all having the same dimension (4 mm wide, 7 mm high, and 1 mm thick), at **f** as-prepared, **g** wet and **h** dry conditions, respectively. Wet refers to the fabrics being immersed in water for 10 min. The pictures (diagrams) on the right illustrate the response of the slit in the three-layer sandwiched hydrogel samples

that of the water uptake (weight change) but to a slightly less extent, which is in line with the trends observed in previous studies [22, 30].

Figure 2d shows representative stress–strain curves of the two hydrogels before and after swelling in water. The HC hydrogel, as expected, has a higher tensile strength and stiffness (modulus) than the LC hydrogel ($p < 0.05$), due to its higher cross-linking density [31–33]. When the hydrogels were swollen in water for 24 h, the Young's modulus and facture strain of the LC hydrogel decreased significantly($p < 0.05$) (Fig. S2), which was expected since its higher water absorption loosens the hydrogel networks [34, 35]; on the other hand, the mechanical properties of the HC hydrogel changed little ($p > 0.05$) (Fig. S2) when immersed in the water as a result of its high cross-linking density and a non-swelling property (Fig. 2c) [34, 36].

Three-layer sandwiched hydrogel composites were produced in a microtome mold (15 mm wide, 7 m high, and 4 mm deep) by means of a step-by-step curing of the two hydrogel solutions. The cross-sectional view of the composite (4 mm wide, 7 mm high, and 1 mm thick) confirmed the sandwich layer structure (Fig. 2e), with the white HC hydrogel forming the inner layer and the transparent LC hydrogel forming the two outer layers, respectively (denoted as LC/HC/LC sandwiched hydrogel composite), which is in contrast to the single-color appearance of the two pure hydrogel samples (Fig. 2a). After this, a 6-mm slit was cut in a central position of each hydrogel sample, with the slit response of the different samples being compared (Fig. 2f). After contacting with water for 10 min, no change was observed in the slits in the two pure samples, except in the case of the swelling of the whole LC hydrogel sample (Fig. 2g, left sample). The three-layer sandwiched hydrogel composite, on the other hand, showed a different response in that the inner HC hydrogel walls bowed apart, resulting in the slit opening (Fig. 2g, right sample). When the samples were dried for 1 h (not completely dry), the inner HC hydrogel walls closed again (Fig. 2h, right). The phenomenon was similar to the pore behavior of leaf stomata (illustrated by the adjacent diagrams), i.e., pore opens when wet and closes when dry, respectively.

Three-Layer Hydrogel Coating on the Fabric Slits

Simulated leaf stomata pores/slits were created by means of a three-layer hydrogel coating on the stretchable knitted

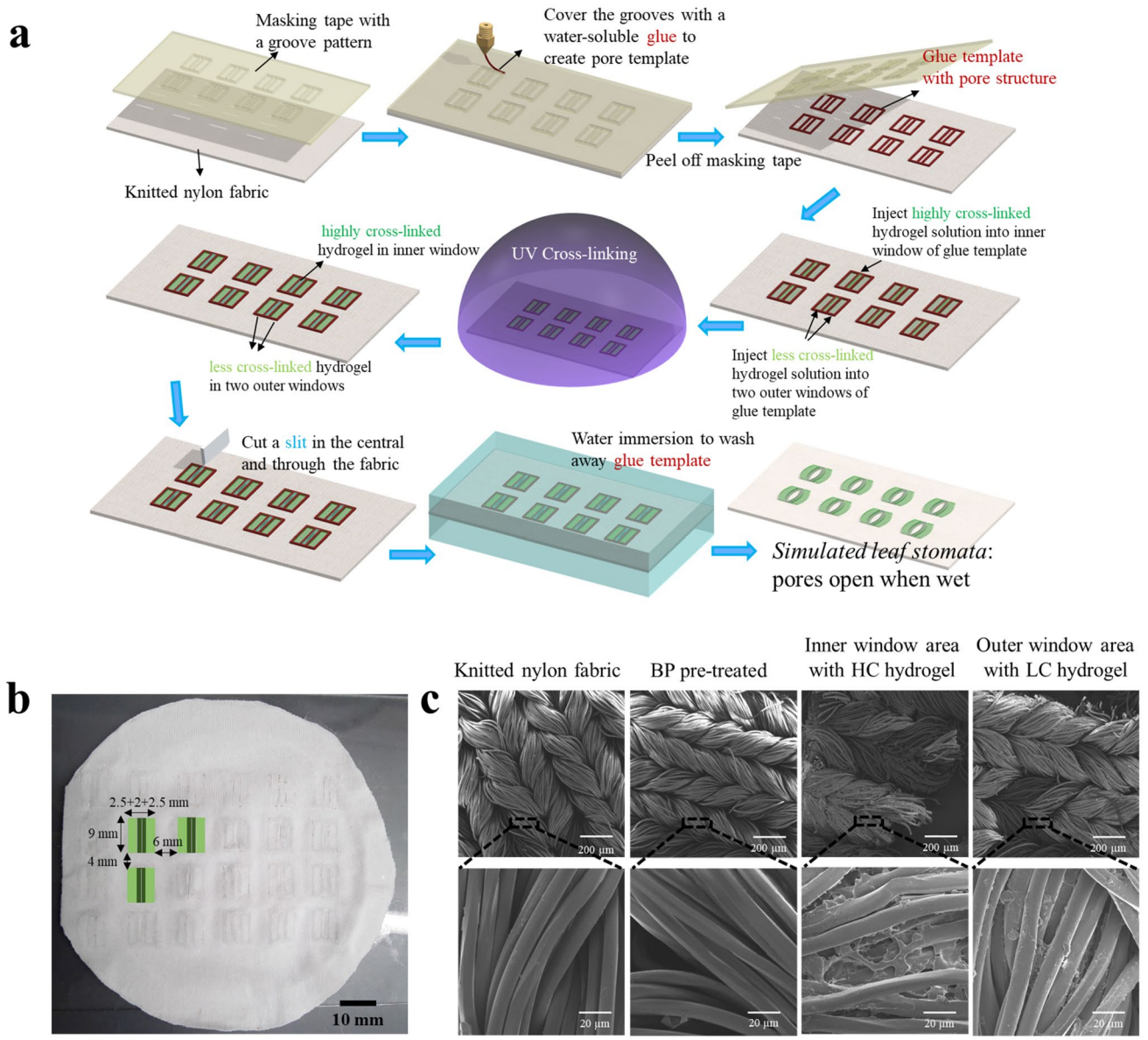

Fig. 3 Fabrication and structure of knitted nylon fabric with slit areas coated with three-layer polyacrylamide (PAAm) hydrogels. **a** Schematic illustration of the procedure of creating simulated stomata pores/slits by means of the three-layer hydrogel coating. **b** A typical fabric with slit areas coated with the three-layer LC/HC/LC PAAm hydrogel, insets illustrate the designed hydrogel coatings and the dimensions and spacings of the three windows in the slit area. **c** SEM morphologies of the control nylon fabric, benzophenone (BP) pre-tread fabric, the inner and outer windows in the three-layer hydrogel coated fabric slit areas

nylon fabric according to the procedure shown in Fig. 3a (also see Fig. S3, for the actual sample procedure). As a first step, the clean fabric was pre-activated by means of a benzophenone (BP)/ethanol solution, in order to create the radical sites for bonding with the polyacrylamide hydrogel [19]. To prevent the wide spread of hydrogel liquid solutions on the fabric, a glue patterned template with three windows (overall 7 mm wide and 9 mm high, with 2-mm wide inner window and two 2.5-mm wide outer windows) was formed on the fabric by pasting and solidifying the glue through a laser-cut tape mask having a groove pattern. The HC hydrogel solution was then poured into the inner window and the LC hydrogel solution into the two outer windows, both then being cured under UV light at 365 nm for 10 min in a sequential order. After curing, a 9-mm slit was cut in the central position of the inner HC hydrogel layer and completely through the fabric, and then the glue solid was washed out in a water bath.

Table 1 Summary of water response when the window areas of the slit (simulated stomata) are coated with different hydrogel combinations at room temperature

Condition	Wet					Dry				
	Outer layer					Outer layer				
Inner layer	Zero (0)	AAm & PAAm (LCP)	AAm (LC)	AAm & PAAm (HCP)	AAm (HC)	Zero (0)	AAm & PAAm (LCP)	AAm (LC)	AAm & PAAm (HCP)	AAm (HC)
Zero (0)	–	+	+	–	–	–	–	–	–	–
AAm & PAAm (LCP)	–			+	+	–			+	–
AAm (LC)	–			+	+	–			+	+
AAm & PAAm (HCP)	–	+ +	+ +[a)]			–	+	–[a)]		
AAm (HC)	–	+ +[a)]	+ +[a,b)]			–	–[a)]	–[a,b)]		

The combinations include zero (0) hydrogel, less cross-linked (LC) hydrogel, highly cross-linked (HC) hydrogel, less cross-linked hydrogel with PAAm (LCP) and highly cross-linked hydrogel with PAAm (HCP)

–, + and + + symbols represent slit close, slightly open, and very open, respectively

[a]Represents good combinations of hydrogels for slit opening and closing

[b]Represents the selected hydrogel combination for the further experiments

The water response of the slits coated with different combinations of less cross-linked (LC) and highly cross-linked (HC) PAAm hydrogels was investigated by immersing the coated fabrics in water for 10 min at room temperature (Table 1, and Fig. S4). The aim of soaking the fabrics was to study the slit response to a situation where the fabric becomes completely wet due to sweating or a wet environment, since under certain circumstances it is desirable that the fabric pores enlarge so as to increase the transmission of moisture and air. Furthermore, the effect of adding PAAm polymer to the cross-linked hydrogel solutions (denoted as LCP for less cross-linked solution with added PAAm polymer and HCP for highly cross-linked solution with added PAAm) was also investigated [18]. It was found the slits (viz. simulated stomata) did not respond to being wet when only the inner window area was coated with either LC, LCP, HC, or HCP hydrogel. Furthermore, the slits opened slightly when only the two outer windows were coated with the LC or LCP hydrogel but did not open when only the two outer windows were coated with the HC or HCP hydrogel. However, when the inner window and the two outer windows were coated with the LC or LCP hydrogel and the HC or HCP hydrogel, respectively, the slits opened slightly when wet, but remained open when they dried. The possible reason for this behavior is that the outer HC or HCP hydrogel takes less time to dry due to lower water uptake (Fig. 2c), and the dried HC or HCP solidifies to fix the shape of the simulated stomata before the inner LCP becomes dry, leading to only a partial closure of the slit. Only when the inner window was coated with the HC or HCP hydrogel and the two outer windows with the LC or LCP hydrogel, the slits opened widely when wet and closed completely when dry (noted as [a)] in Table 1). Adding PAAm polymer made little difference. In fact, it even retarded the closure of the slits for the LCP/HCP/LCP hydrogel coated sample (viz. HCP hydrogel coated inner window and LCP hydrogel coated two outer windows). Therefore, the LC/HC/LC combination (viz. HC for the inner and LC for the two outer windows) was selected for the following experiments, as noted [b)] in Table 1.

Figure 3b showed a typical nylon fabric with the slit window areas (7 mm wide and 9 mm high) coated with the three-layer LC/HC/LC PAAm hydrogel, which maintained a flat surface without buckling. The spacings between each slit area were 6 mm and 4 mm in in horizontal and vertical directions, respectively. The hydrogels have fully covered the templated window areas of the fabrics, since the areas were made completely wet by the hydrogel spreading after it was injected (Fig. S3f). The thickness of the hydrogel-coated area was 0.42 ± 0.01 mm, as compared to 0.39 ± 0.01 mm for the control nylon fabric. Figure 3c shows the SEM morphologies of the knitted nylon fabric before and after being coated with the hydrogel. The fibers of both the control fabric and the BP pre-treated fabric had a smooth surface, while the fibers in the window areas coated with hydrogels had a relatively rough appearance, with the hydrogel creating integrated bonds. It was apparent that the hydrogel coating on the fiber surface was not perfectly smooth and homogenous, but that it had penetrated across the fabric (Fig. S5a), as the back window areas exhibited a similar rough appearance (Fig. S5b). The HC hydrogel coated inner window area and the LC hydrogel coated outer window area exhibited a similar fiber surface appearance.

Performance of Fabrics with Three-Layer Hydrogel Coated Slits

The water response of the nylon fabrics with the slit window areas coated with the three-layer LC/HC/LC PAAm hydrogels was investigated in terms of dimensional changes as well as water vapor transmission and air permeability. When in contact with water for 10 min at room temperature, the slits in the sample were found to open widely (Fig. 4a, left). According to the optical images, the slit width increased to an average of 0.72 ± 0.26 mm (Fig. S6a, i), the largest slit reaching around 1.30 mm, compared to 0.20 mm for the as-prepared fabric slits. When dried for 1 h at room temperature, the slits on the fabric closed to a width (opening) of 0.20 ± 0.07 mm (Fig. 4a, right, and Fig. S6a), which was similar to the original size. The original fabric (viz. control) and fabric with slits only (viz. no coating) did not respond when contacting with the water (Fig. S6). The opening and closing behavior of the simulated stomata changed very little during 20 wet and dry alternation cycles, indicating excellent durability of its functionalities.

Apart from water, the slit response to artificial sweat of the control fabric with slits only (viz. no coating) and the fabric with the slit window areas coated with the three-layer PAAm hydrogels was investigated. The slits of the control fabric did not show any response when in contact with or immersed for 10 min in the artificial sweat (Movie S1 and Fig. S7a). From the Movie S2, we can see the hydrogel coated slits started to open almost instantaneously (in ~ 10 s) when in contact with the artificial sweat, and largely maintained their open status after being immersed in the artificial sweat for 1 min and 10 min, respectively (Movie S2 and Fig. S7c). When completely dry, the slits closed once again (Fig. S7d). The deformation and response of the hydrogel coated slits to artificial sweat were almost the same as that in pure water (Fig. 4a). It is worth noting that, the above experiment on the slit response to artificial sweat was conducted after the fabric samples were placed in a dry laboratory environment (20 ± 2 °C temperature, 65 ± 2% relative humidity) for over 1 year, whereas the slit response to pure water was conducted 1 year before. The almost same response of

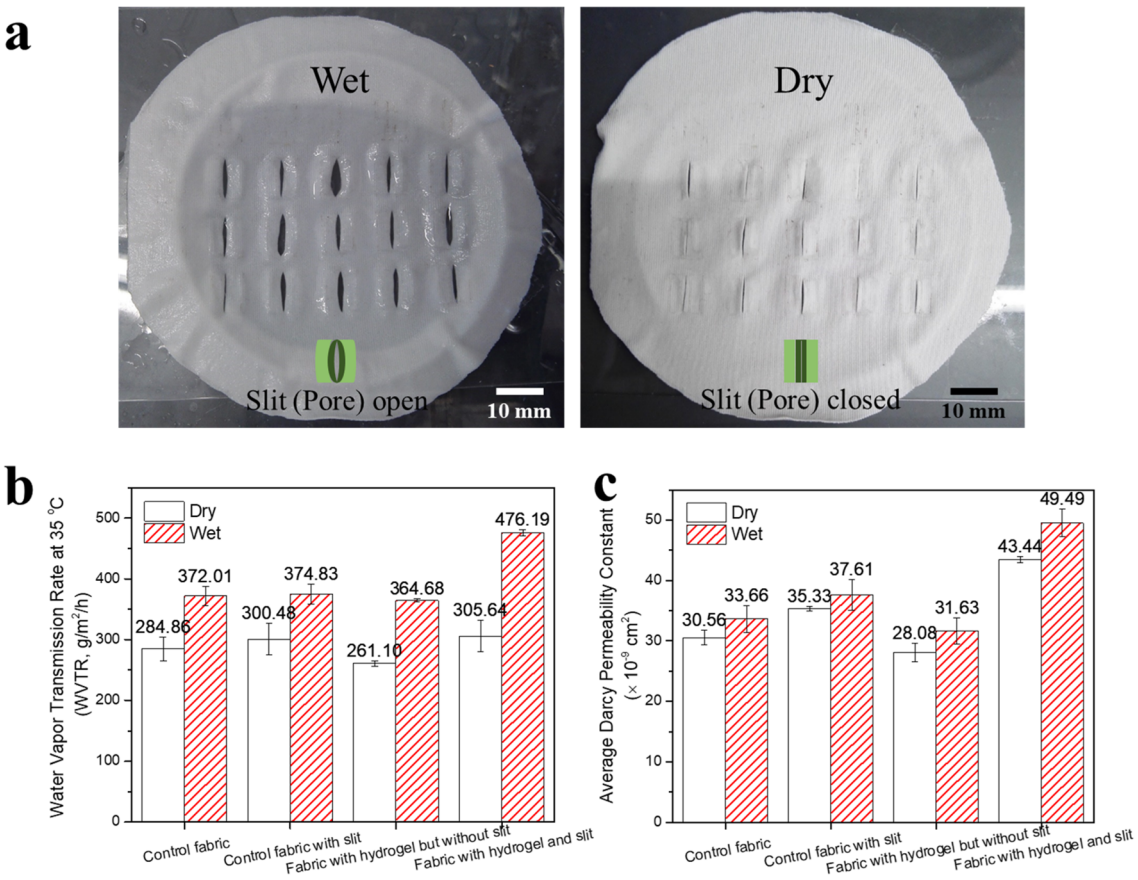

Fig. 4 The effect of the response of the slit areas coated with three-layer PAAm hydrogels on the water vapor transmission and air permeability of the knitted nylon fabrics. **a** Photo images of a knitted nylon fabric with the slit areas coated with three-layer LC/HC/LC PAAm hydrogels under wet (left) and dry (right) conditions, respectively; inset illustrates the slit response. b Water vapor transmission rates at 35 °C and **c** air permeability at room temperature for control nylon fabric, control fabric with slits only, fabric coated with three-layer hydrogels but without slits, and fabric with both hydrogels and slits under both dry and wet conditions, respectively

the artificial stomata to artificial sweat (tested 1 year after) and to pure water (tested 1 year before) demonstrated the excellent durability of the "open-close" behavior of artificial stomata to water absorption/desorption. Furthermore, the response rate of the simulated stomata to water or sweat can be adjusted by changing the formulation of the less cross-linked (LC) hydrogel and/or that of the highly cross-linked (HC) hydrogel, so that they will exhibit different swelling ratio and volume expansion.

The breathability in terms of water vapor transmission and air permeability of the designed nylon fabric with the three-layer hydrogel coated slits was evaluated. Water vapor transmission rate (WVTR) was evaluated by means of the cup method (BS7209 standard) [24, 25] at a temperature of 35 °C to simulate the temperature of the human skin (Fig. S8a) [37, 38]. The control nylon fabrics with and without cut slits and the fabric with hydrogel coating but without slits were also tested (Fig. S8b–d). As shown in Fig. 4b, the dry fabrics with the cut slits (15 slits cut in a 90-mm circular fabric sample) regardless of hydrogel coating had a slightly higher WVTR compared with the dry control sample (300–306 g/m^2/h vs. 285 g/m^2/h). This was due to the cut slits in the fabrics, even though the slits were nominated "closed", their gap of 0.20 mm (Fig. S6a, f) was still much larger than the original pores between yarns (Fig. S6d) and could possibly accelerate the transmission rate. The fabric with the hydrogel coating but without the slits exhibited the lowest transmission rate (261 g/m^2/h) of all the samples ($p < 0.05$), due to the hydrogel coating in the window area by blocking the gaps between the yarns and thereby retarding or greatly reducing the moisture transmission [39–41]. All the fabrics increased the vapor transmission rate when wet, due to the surface evaporation of the vapor. Nevertheless, compared to the two control fabric samples (372 and 375 g/m^2/h) and the sample with the hydrogel coating but without any cut slits (365 g/m^2/h), the sample with the hydrogel coating and cut slits exhibited a significant higher (56% higher) vapor transmission (477 g/m^2/h) ($p < 0.05$) under dry conditions. Clearly, the opening of the slits when wet (Fig. S8i) greatly increased the transmission of vapor, exceeding the effect of the hydrogel blocking. Therefore, the results showed the presence and dimensions of the slits, which are larger than the pores of the fabric, play an important role in regulating the moisture transmission properties of the fabric when wet.

Finally, the air permeability, the convective heat transfer during thermal regulation, was measured by means of a gas permeability module on a Capillary Flow Porometer [26]. As for the WVTR test, an 18.3-mm circular fabric sample with two cut slits coated with three-layer hydrogels was tested both under dry and wet conditions at room temperature, and the results were compared to those of 3 control fabrics, namely the original fabric and the fabric with two cut slits only, as well as the hydrogel coated fabric but without slits (Fig. S9). An average Darcy's Permeability Constant for each testing sample was calculated based on the sample thickness and diameter, and the air flow and pressure. As can be seen in Fig. 4c, the Darcy's Permeability Constant showed a similar trend as that of the WVTR results, i.e., the fabric with cut slits coated with the three-layer hydrogels had a higher permeability ($> 43 \times 10^{-9}$ cm^2) compared to that of both control fabrics and the fabric with hydrogel but without slits ($< 38 \times 10^{-9}$ cm^2). This applied to both the dry or wet condition ($p < 0.05$). The wet fabric had a higher air permeability ($\sim 50 \times 10^{-9}$ cm^2) than the dry fabric (43×10^{-9} cm^2) ($p < 0.05$), thereby proving that the opening of the pores/slits greatly improved the air flow through the fabric, and consequently also the fabric breathability and heat transfer.

Discussion

While a resting person usually produces ~ 30 g/m^2/h insensible perspiration, it can be as high as ~ 1000 g/m^2/h sweat during physical activities [38]. In order to maximize thermal comfort and barrier protection, it is therefore highly desirable to design smart fabric materials, the vapor and air permeability of which can change according to the body's physiological and external conditions [42].

In this study, a novel fabric was developed which has environmental-responsive permeability. This was achieved by creating leaf stomata-mimicking water responsive pores (cut slits) in the fabric, where the pores/slits are coated with a specific pattern of highly cross-linked (HC) and less cross-linked (LC) PAAm hydrogels. The hydrogel coated pores/slits act like leaf stomata, which open under wet and close under dry conditions. To construct the special hydrogel pattern, the precise attachment of each hydrogel material in its designated position in the fabric is key. To do so, a photo-initiator, benzophenone was used as a bonding agent, due to its oxygen inhibition effect, which provided radical sites on the fabric for robust reaction with the UV-curable hydrogel monomers [19]. For selective coating in the desired areas, glue templates were used in order to prevent the spreading of the hydrogel solution. For a knitted nylon fabric containing the designed simulated leaf stomata, the outer highly swellable LC hydrogel layer functions as the driver of the "guard cells", which swell greatly under wet conditions. Due to the linkage with the inner less swellable HC hydrogel, the dimensions of the "guard cells" change asymmetrically during the swelling, i.e., the outer LC layers swell far more than the inner HC layers, resulting in the outward bending of the two "guard cells". Since the knitted fabric substrate is very stretchable and firmly bonded to the hydrogel network via BP pre-treatment, the outward bending of the "guard cells" bowed the walls of the slit apart, leading to its

opening. Though the hydrogel coating could slightly retard the moisture transmission [39–41], the opening/enlargement of the pores/slits under wet conditions significantly increased the moisture transmission of the fabric to 477 g/m^2/h at 35 °C, being 56% higher than that under dry conditions when the pores/slits are closed, and 100% higher than that of the reported Nafion™ (perfluorosulfonic acid ionomer) film shirt with semilunar flipping patterns (237 g/m^2/h) [6]. This unique property of the fabric with simulated leaf stomata (viz. hydrogel coated slits) will greatly facilitate sweat evaporation under profuse sweating conditions and this effect would be further enhanced by body movement and/or by wind. Conversely, when the fabric dries out, the water evaporation causes the swollen hydrogels back to their original unswollen dimensions and hence the pores/slits to close again. As there is no bending, there is little effect on the air permeability.

The opening and closing behaviors of the simulated leaf stomata in the developed fabric will be very beneficial to personal moisture and thermal management under different physiological and environmental conditions. For example, when a wearer is resting under normal/dry conditions, the simulated stomata remain closed in order to retain the heat and maximize the barrier protection. Conversely, when the wearer is sweating profusely either during active sports or exposure to hot and humid conditions, particularly wet conditions, the pores/slits of the fabric will be opening in order to increase the heat and moisture permeability and thereby thermal comfort. This is also the reason why water immersion instead of moisture was used in an attempt to mimic the severe sweating conditions where the wearer's skin could be covered by a layer of water (sweat). Liquid water was used as the substitute of sweat in most of the experiments since the response of the PAAm hydrogel to water is the same as that to the artificial sweat (Figs. 4a and S7c, d), as the PAAm hydrogel not having any surface charges, hence being unaffected by the electrolytes in the sweat.

Apart from the nylon fabric, a cotton fabric and a polyurethane fabric were also used to demonstrate the feasibility of the proposed concept after being pre-activated by benzophenone (BP) initiator and coated with the three-layer hydrogel on their cut slits. As shown in Fig. S10, both fabrics displayed opening and closing behaviors on the slits under wet and dry conditions, respectively, similarly as that on the nylon fabric (Fig. 4a), demonstrating our proposed strategy can be applicable in different materials. It is also believed that the same effect can be achieved with other materials, such as polyester, linen and wool, as long as they are pretreated by a bonding agent, such as the BP initiator used in this work to enable the hydrogel coating to adhere to the fabric.

The present design of water responsive simulated leaf stomata can be further modified by reducing the stomata dimensions and automating the hydrogel coatings on the surface of the fabric or membrane. If the pore/slit dimension is reduced to a micro- size, the fabric or membrane would have a greater barrier protection and hence the heat retention and water repellency when the pores/slits are closed [43], and the size of the opening slits/pores might also be more controllable. While cutting slits in the fabric may adversely affect its mechanical properties to some extent, it should be acceptable as laser cut slits are very common in sportswear and fashion apparel [44]. In future, one can also consider creating the holes or slits during the fabric manufacturing process and treat their adjacent areas with the responsive hydrogel materials in order to eliminate any potential problems related to the mechanical properties of the fabric. Finally, to commercialize the new development, it is also desirable to scale up the coating process, which could possibly be achieved by means of either screen or digital printing, which would also greatly simplify the process by depositing the hydrogels in the desired regions without the need for the pre-templating procedure.

Conclusion

In conclusion, it can be stated that an environmental responsive smart fabric has been developed in which simulated leaf stomata pores/slits were created in a commercial knitted nylon fabric, with the inner windows of the slit areas being coated with a highly cross-linked (HC) less swellable PAAm hydrogel, and the two outer windows of the slits with a less cross-linked (LC) highly swellable hydrogel. Because of the different swelling behavior of the two hydrogels, the slits act as simulated leaf stomata, which open under wet conditions and close under normal/dry conditions. The hydrogel coating in the slit areas was investigated by means of SEM images, while the opening and closing behavior of the slits was studied using optical imaging. The slit response to artificial sweat was the same as that to water. Due to the opening of the pores/slits under wet conditions, both vapor transmission and air permeability increased significantly for the developed fabric. This smart fabric can have applications in functional clothing to maximize thermal comfort under changing and extreme physiological and environmental conditions. Furthermore, the concept can be extended to other responsive membranes, such as wound dressings, controlled drug and nutrient release, and various other relevant industrial products.

Supplementary Information The online version contains supplementary material available at https://doi.org/10.1007/s42765-023-00269-5.

Acknowledgements This work was supported by Prof. Fan's Faculty Startup Fund of the College of Human Ecology, Cornell University. This work made use of the facilities of the Cornell Center for Materials Research (CCMR) supported by the National Science Foundation under Award Number DMR-1719875. The authors also acknowledge Dr. Xia Zeng for equipment guidance and support, Charles V. Beach and Vincent Chicone for their assistance with the mask fabrication. Finally, the PI, Prof. Fan would like to acknowledge the funding support of RGC GRF project #15213920 and Hong Kong Polytechnic University Project of Strategic Importance #ZE1H for further analysis of the experimental data and improvement of the manuscript.

Author Contributions All the authors contributed to the writings of the manuscript and have approved the final version of the manuscript.

Data availability The data sets generated and/or analyzed in this study are available from the corresponding author on reasonable request.

Declarations

Conflict of Interest The authors declare no conflicting financial or other interests.

References

1. Leng XQ, Hu XY, Zhao WB, An BG, Zhou X, Liu ZF. Recent advances in twisted-fiber artificial muscles. *Adv Intell Syst*. **2021**;*3*:2000185.
2. Sun Z, Cao Z, Li Y, Zhang Q, Zhang X, Qian J, Jiang L, Tian D. Switchable smart porous surface for controllable liquid transportation. *Mater Horiz*. **2022**;*9*:780.
3. Yu Y, Zheng G, Dai K, Zhai W, Zhou K, Jia Y, Zheng G, Zhang Z, Liu C, Shen C. Hollow-porous fibers for intrinsically thermally insulating textiles and wearable electronics with ultrahigh working sensitivity. *Mater Horiz*. **2021**;*8*:1037.
4. Xu DW, Ouyang ZF, Dong YJ, Yu HY, Zheng S, Li SH, Tam KC. Robust, breathable and flexible smart textiles as multifunctional sensor and heater for personal health management. *Adv Fiber Mater*. **2022**. https://doi.org/10.1007/s42765-022-00221-z.
5. Zhong Y, Zhang FH, Wang M, Gardner CJ, Kim G, Liu YJ, Leng JS, Jin S, Chen RK. Reversible humidity sensitive clothing for personal thermoregulation. *Sci Rep*. **2017**;*7*:44208.
6. Mu J, Wang G, Yan H, Li H, Wang X, Gao E, Hou C, Pham ATC, Wu L, Zhang Q, Li Y, Xu Z, Guo Y, Reichmanis E, Wang H, Zhu M. Molecular-channel driven actuator with considerations for multiple configurations and color switching. *Nat Commun*. **2018**;*9*:590.
7. Wang W, Yao LN, Cheng CY, Zhang T, Atsumi H, Wang LD, Wang GY, Anilionyte O, Steiner H, Ou JF, Zhou K, Wawrousek C, Petrecca K, Belcher AM, Karnik R, Zhao XH, Wang DIC, Ishii H. Harnessing the hygroscopic and biofluorescent behaviors of genetically tractable microbial cells to design biohybrid wearables. *Sci Adv*. **2017**;*3*: e160198.
8. Kim G, Gardner C, Park K, Zhong Y, Jin SH. Human-skin-inspired adaptive smart textiles capable of amplified latent heat transfer for thermal comfort. *Adv Intell Syst*. **2020**;*2*:2000163.
9. Li XQ, Ma BR, Dai JY, Sui CX, Pande D, Smith DR, Brinson LC, Hsu PC. Metalized polyamide heterostructure as a moisture-responsive actuator for multimodal adaptive personal heat management. *Sci Adv*. **2021**;*7*:eabj7906.
10. Jia TJ, Wang Y, Dou YY, Li YW, de Andrade MJ, Wang R, Fang SL, Li JJ, Yu Z, Qiao R, Liu ZJ, Cheng Y, Su YW, Minary-Jolandan M, Baughman RH, Qian D, Liu ZF. Moisture sensitive smart yarns and textiles from self-balanced silk fiber muscles. *Adv Funct Mater*. **2019**;*29*:1808241.
11. Hu XY, Leng XQ, Jia TJ, Liu ZF. Twisted and coiled bamboo artificial muscles for moisture responsive torsional and tensile actuation. *Chin Phys B*. **2020**;*29*: 118103.
12. Khan AQ, Yu KQ, Li JT, Leng XQ, Wang ML, Zhang XS, An BG, Fei B, Wei W, Zhuang HC, Shafiq M, Bao LL, Liu ZF, Zhou X. Spider silk supercontraction-inspired cotton-hydrogel self-adapting textiles. *Adv Fiber Mater*. **2022**;*4*:1572.
13. Pennisi E. EVOLUTION How plants learned to breathe even early plants likely had sophisticated pores to regulate water and swap gases with their environment. *Sci*. **2017**;*355*:1110.
14. Christodoulakis NS, Menti J, Galatis B. Structure and development of stomata on the primary root of *Ceratonia siliqua* L. *Ann Bot*. **2002**;*89*:23.
15. Lange OL, Losch R, Schulze ED, Kappen L. Responses of stomata to changes in humidity. *Planta*. **1971**;*100*:76.
16. Roelfsema MRG, Hedrich R. In the light of stomatal opening: new insights into "the Watergate." *New Phytol*. **2005**;*167*:665.
17. Lao LH, Robinson SS, Peele B, Zhao HC, Mac Murray BC, Min JK, Mosadegh B, Dunham S, Shepherd RF. Selective mineralization of tough hydrogel lumens for simulating arterial plaque. *Adv Eng Mater*. **2017**;*19*:1600591.
18. Li S, Peele BN, Larson CM, Zhao HC, Shepherd RF. A stretchable multicolor display and touch interface using photopatterning and transfer printing. *Adv Mater*. **2016**;*28*:9770.
19. Yuk H, Zhang T, Parada GA, Liu XY, Zhao XH. Skin-inspired hydrogel-elastomer hybrids with robust interfaces and functional microstructures. *Nat Commun*. **2016**;*7*:12028.
20. Butler MF, Clark AH, Adams S. Swelling and mechanical properties of biopolymer hydrogels containing chitosan and bovine serum albumin. *Biomacromol*. **2006**;*7*:2961.
21. Odent J, Wallin TJ, Pan WY, Kruemplestaedter K, Shepherd RF, Giannelis EP. Highly elastic, transparent, and conductive 3D-printed ionic composite hydrogels. *Adv Funct Mater*. **2017**;*27*:1701807.
22. Ren P, Zhang H, Dai Z, Ren F, Wu Y, Hou R, Zhu Y, Fu J. Stiff micelle-crosslinked hyaluronate hydrogels with low swelling for potential cartilage repair. *J Mater Chem B*. **2019**;*7*:5490.
23. Lao L, Shou D, Wu YS, Fan JT. "Skin-like" fabric for personal moisture management. *Sci Adv*. **2020**;*6*:eaaz0013.
24. Huang JH, Qian XM. Comparison of test methods for measuring water vapor permeability of fabrics. *Text Res J*. **2008**;*78*:342.
25. Kim M, Wu YS, Kan EC, Fan J. Breathable and flexible piezoelectric ZnO@PVDF fibrous nanogenerator for wearable applications. *Polymer*. **2018**;*10*:745.
26. Fernando JA, Chung DDL. Pore structure and permeability of an alumina fiber filter membrane for hot gas filtration. *J Porous Mater*. **2002**;*9*:211.
27. Ramadan Y, Gonzalez-Sanchez MI, Hawkins K, Rubio-Retama J, Valero E, Perni S, Prokopovich P, Lopez-Cabarcos E. Obtaining new composite biomaterials by means of mineralization of

methacrylate hydrogels using the reaction-diffusion method. *Mater Sci Eng C-Mater Biol Appl*. **2014**;*42*:696.
28. Wong RS, Ashton M, Dodou K. Effect of crosslinking agent concentration on the properties of unmedicated hydrogels. *Pharmaceutics*. **2015**;*7*:305.
29. Xu B, Liu Y, Wang L, Ge X, Fu M, Wang P, Wang Q. High-strength nanocomposite hydrogels with swelling-resistant and anti-dehydration properties. *Polymers (Basel)*. **2018**;*10*:1025.
30. Peng L, You M, Yuan Q, Wu C, Han D, Chen Y, Zhong Z, Xue J, Tan W. Macroscopic volume change of dynamic hydrogels induced by reversible DNA hybridization. *J Am Chem Soc*. **2012**;*134*:12302.
31. Liu RQ, Liang SM, Tang XZ, Yan D, Li XF, Yu ZZ. Tough and highly stretchable graphene oxide/polyacrylamide nanocomposite hydrogels. *J Mater Chem*. **2012**;*22*:14160.
32. Huang YP, Zhang BP, Xu GW, Hao WT. Swelling behaviours and mechanical properties of silk fibroin-polyurethane composite hydrogels. *Compos Sci Technol*. **2013**;*84*:15.
33. Gao G, Du G, Sun Y, Fu J. Self-healable, tough, and ultrastretchable nanocomposite hydrogels based on reversible polyacrylamide/montmorillonite adsorption. *ACS Appl Mater Interfaces*. **2015**;*7*:5029.
34. Kamata H, Akagi Y, Kayasuga-Kariya Y, Chung U, Sakai T. "Nonswellable" hydrogel without mechanical hysteresis. *Sci*. **2014**;*343*:873.
35. Chen H, Yang FY, Hu RD, Zhang MZ, Ren BP, Gong X, Ma J, Jiang BB, Chen Q, Zheng J. A comparative study of the mechanical properties of hybrid double-network hydrogels in swollen and as-prepared states. *J Mater Chem B*. **2016**;*4*:5814.
36. Li SZ, Zhou D, Pei MJ, Zhou YS, Xu WL, Xiao P. Fast gelling and non-swellable photopolymerized poly (vinyl alcohol) hydrogels with high strength. *Eur Polym J*. **2020**;*134*:109854.
37. Bierman W. The Temperature of the Skin Surface. *J Am Med Assoc*. **1936**;*106*:1158.
38. Fan JT, Chen YS. Measurement of clothing thermal insulation and moisture vapour resistance using a novel perspiring fabric thermal manikin. *Meas Sci Technol*. **2002**;*13*:1115.
39. Wang XW, Hu HW, Yang ZY, He L, Kong YY, Fei B, Xin JH. Smart hydrogel-functionalized textile system with moisture management property for skin application. *Smart Mater Struct*. **2014**;*23*: 125027.
40. Li B, Li DP, Yang YN, Zhang L, Xu K, Wang JP. Study of thermal-sensitive alginate-Ca2+/poly(N-isopropylacrylamide) hydrogels supported by cotton fabric for wound dressing applications. *Text Res J*. **2019**;*89*:801.
41. Bashari A, Nejad NH, Pourjavadi A. Effect of stimuli-responsive nano hydrogel finishing on cotton fabric properties. *Indian J Fibre Text Res*. **2015**;*40*:431.
42. Kamalha E, Zeng YC, Mwasiagi JI, Kyatuheire S. The comfort dimension; a review of perception in clothing. *J Sens Stud*. **2013**;*28*:423.
43. Mukhopadhyay A, Midha VK. A review on designing the waterproof breathable fabrics part i: fundamental principles and designing aspects of breathable fabrics. *J Ind Text*. **2008**;*37*:225.
44. McQuerry M, Hogans K. Assessment of ventilated athletic uniforms for improved thermal comfort. *AATCC J Res*. **2018**;*5*:1.

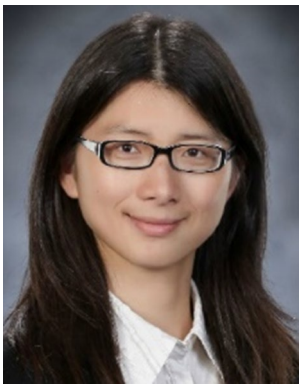

Dr. Lihong Lao is currently a postdoctoral research associate in Department of Materials Science and Engineering at University of Illinois Urbana-Champaign. She received her Ph.D. in Fiber Science (Materials Science and Engineering) from Cornell University in 2019, and M.S. and B.S. in Polymer Science and Engineering from Zhejiang University in 2010 and 2007. Her research focuses on functional polymeric materials and smart systems with tailored surface chemistries and properties for applications ranging from fibrous systems, smart textiles to biomedical products.

Dr. Hedan Bai is currently a postdoctoral fellow in the Querrey Simpson Institute for Bioelectronics at Northwestern University. She received her Ph.D. in Mechanical Engineering from Cornell University in 2021. Previously, she received her B.S. degree from Cornell University in 2016 in both Mechanical and Aerospace Engineering, and Operations Research and Information Engineering. Her research focuses on the design and fabrication of soft optical sensors, miniature soft robots and bioelectronics.

Prof. Jintu Fan holds Ph.D from Leeds University (1989) and BSc from Donghua University (1985). He is currently Lee family Professor in Textiles Technology and Chair Professor of Fiber Science and Apparel Engineering at School of Fashion and textiles, Hong Kong Polytechnic University (PolyU). Professor Fan is a Former Head of Institute of Textiles and Clothing at PolyU (2018–2022) and Former Department Chair and Vincent VC Woo Professor in Fiber Science and Apparel Design at Cornell University (2012–2018).